Algerian Journal of Chemical Engineering

ISSN:2773-3068

Journal homepage: http://www.ajce.periodikos.com.br/

Original Article

Kinetics, equilibrium and thermodynamics studies of congo red dye adsorption from aqueous solution onto activated cowpea (*Vigna unguiculata)* husk

Abdullahi Muhammad Ayuba and Bridget Idoko*

Department, of Pure and Industrial Chemistry, Bayero University, Kano, Nigeria

ARTICLE INFO

Article history:
Received 14 June 2021
Revised 09 September 2021
Accepted 10 October 2021

Keywords:
Adsorption
Congo Red
Isotherms
Kinetics
Vigna unguiculata

ABSTRACT

Adsorption of Congo red (CR) dye from aqueous solution onto activated cowpea husk (ACPH), a low-cost agricultural waste material in a batch process was investigated. Adsorption was studied as a function of amount of adsorbent, pH, initial dye concentration and time. It was found that adsorption capacity varied linearly with the amount of adsorbent, initial CR concentration with time. The results show that maximum adsorption capacity was obtained at the optimum levels of contact time (24.3157mg/g at 60 minutes), adsorbent dose (24.532mg/g at 0.1g), initial dye concentration (407.2787mg/g at 500mg/L) and pH (24.26mg/g at 1.5). Adsorption equilibrium data were represented by isotherm, kinetics and thermodynamics models. Three isotherm models namely Langmuir, Freundlich and Temkin were tested and adsorption was found to fit well into Langmuir model relatively better than others. The maximum loading capacity (q_m) of the adsorbent for Congo red obtained from the Langmuir isotherm model is 263.16 mg/g. The kinetic data was well described by the pseudo-second order kinetic model with the correlation coefficients (R^2) value of 0.994. The adsorption process was found to be thermodynamically endothermic and spontaneous. The negative value of ΔS (-0.00053J/mol.k) infer that the randomness decreases at the adsorbent/adsorbate interface during the adsorption process. FTIR and SEM analyses of the adsorbent suggest that adsorption of the dye was through an electrostatic interaction between the functional groups present in the dye and those on the surface of the adsorbent.
.

1. Introduction

Dyes are coloured substances that can be applied to various substrates (textile materials, leather, paper, hair) from a liquid in which they are completely, or at least partly, soluble. Man has made use of dyes since prehistoric times, and in fact, the demand and the usage of dyes have continuously increased. However, the presence of dyes even in trace quantities is very undesirable in aqueous environment as they are generally stable to light and oxidizing agents, and are resistant to aerobic digestion [1]. This is partly due to the realization that contamination of aquatic environment by dyes causes reduction in the growth of algae due to obstruction of light required for photosynthesis, which subsequently leads to ecological imbalance in the aquatic ecosystem [2].

Congo red ($C_{32}H_{22}N_6Na_2O_6S_2$: disodium 4-amino-3-[4-[4-(1-amino-4-sulfonato-naphthalen-2-yl) diazenylphenyl]phenyl]diazenyl-naphthalene-1-sulfonate) is a secondary diazo dye that is used in textile, paper, and leather industries. It is a water-soluble dye and can be used as a pH indicator due to its colour change from blue to red at pH 3.0 – 5.2. The coloured effluents which are discharged into water cause environmental pollution with harmful effects on aquatic life [3]. Many researchers have studied the removal of this carcinogenic dye through adsorption process using various adsorbents of plant origin including: coconut residual fiber [4], *Phoenix dactylifera* date stones and *Ziziphus lotus* jujube shells [5], *Solanum tuberosum* and *Pisum sativum* peels [6], common Beach (*Fagus sylvatica L.*) [7], *Ulva lactuca* biomass [8], Mango leaves [9], Litchi peel biochar [10], Pomelo peel [11], Brewer's grains [12], Magnolia-leaf [13], Pineapple peel [14], Banana peel [15], Walnut shell [16], Pine bark [17],

* *Corresponding author.* Tel.: 07065654046
E-mail address:bridgetidoko0803@gmail.com
http://dx.doi.org/ 10.5281/zenodo.5670200

Vetiveria zizanioides [18], and Cabbage waste [19].

However, the adsorption process is influenced by the nature of the adsorbate and its substituent groups. The presence and concentration of surface functional groups play an important role in the adsorption capacity and the removal mechanism of the adsorbate. The most commonly used adsorbent in the adsorption process is activated carbon. Activated carbon has the advantage of exhibiting a high adsorption capacity for colour pollutants due to their high surface area and porous structure [20].

Vigna Unguiculata (Cowpea) is a versatile African crop; it feeds people and their livestock. It is a high protein food and very popular in West Africa. As a nitrogen fixing legume, Cowpea improves soil fertility and consequently helps to increase the yields of cereal crops when grown in rotation. It is referred to as the "hungry season crop" given that it is the first crop to be harvested before the cereal crops are ready. It is a crop that offers farmers great flexibility. They can choose to apply more input and pick more beans or- if cash and inputs are scarce, they can pick fewer beans and allow the plants to produce more foliage [21]

This research is aimed at investigating the kinetics, thermodynamics and equilibrium isotherms of Congo red removal from aqueous solution by adsorption onto activated cowpea husk.

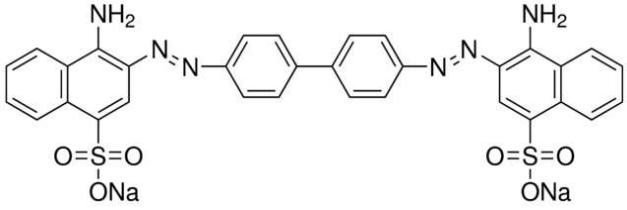

Fig 1. Structure of Congo red dye

2. Materials and Methods

2.1 Adsorbent Collection and Preparation

The cowpea husk (CPH) was obtained from a local market in Kano, Nigeria. The shells obtained after removing the seeds from the pods was washed and air dried by removing the bean seeds. CPH was first washed with water to remove dirt from its surface and subsequently dried at 105° C for 24 hrs in an oven to remove the moisture content. Methods used were largely without modification for the preparation of the activated carbon [22-23]. 60g of the cowpea husk was mixed with 50ml of 10% phosphoric acid (H_3PO_4). The treated samples were pyrolyzed at 450°C for 1 h in an electric muffle furnace. After activation, the mixture was removed from the furnace and allowed to cool to room temperature. The pyrolyzed sample was washed with 2% HCl (v/v) several times and then with distilled water until a neutral pH was achieved. Later the carbon paste was dried in an electric oven at 105°C for 24 h. The carbon preparation experiments were carried out several times to obtain enough activated carbon samples for further analysis and characterization. The resulting activated carbon was kept in air-tight container and labelled AC-CPH (Activated Carbon Cowpea husk) for subsequent usage.

2.2 Preparation of Congo Red solution

The Stock solution (Congo Red (CR) dye) was prepared by dissolving accurately weighed 1g of the dye into a 1L to produce 1000 mgL^{-1}using distilled water. The experimental solutions (50-500mg/L of desired concentration were prepared accordingly by diluting the stock solution with distilled water [24]. The concentration of the residual un-adsorbed CR dye was measured at λ_{max} = 498.3 nm using UV–Visible spectrophotometer (Model Hitachi 2800).

2.3 Characterization of the Adsorbent

The surface morphological properties of the adsorbent sample were investigated using Scanning Electron Microscope (SEM, Phenom World Eindhoven). Scanned micrographs of adsorbents before and after adsorption were taken at an accelerating voltage of 15.00 kV and x500 magnification. FTIR analyses of the CR dye, adsorbents before and after adsorption were carried out using Cary 630 Fourier Transform Infrared Spectrophotometer Agilent Technology. The analysis was done by scanning the sample through a wave number range of 650 – 4000 cm^{-1}; 32 scans at 8cm^{-1}resolution.

2.4 Batch Adsorption Experiment

Batch experiments were carried out to determine the optimum conditions for the equilibrium adsorption of Congo red onto activated cowpea husk. The results obtained after the optimization experiments were used to conduct the batch adsorption experiments. Each of these systems was separately run in a 250 cm^3 conical flask differently at 30^0, 40^0, 50^0 and 60^0C respectively. The conical flasks were covered during the equilibration period and placed on a temperature-controlled tightly Innova 4000 incubator shaker for the earlier reported period. After reaching adsorption equilibrium, the content was filtered through Whatman No 1 filter paper. The filtrate was analysed using Perkin-Elemer Uv-visible spectrophotometer at maximum absorbance wavelength of 498.3nm [24]. The extent of adsorption was calculated using equations (1) and (2) respectively:

$$Q_e = \frac{(Co-Ce)}{m} \times V \qquad (1)$$

$$R_{em}(\%) = \frac{(Co-Ce)}{Co} \times 100 \qquad (2)$$

Where Q_e is the adsorption capacity (mg/g), C_o and C_e are the initial and final equilibrium concentration (mg/l) of Congo red in solution, V is the volume of Congo red in solution (L), and *m* is the mass (g) of the adsorbent.

3. Results and Discussion

3.1 FTIR Spectroscopy and Scanning Electron Micrograph

FTIR analysis spectrum as shown in Fig. 2 of the adsorbent before and after adsorption was carried out using Cary 630 Fourier Transform Infrared Spectrophotometer Agilent Technology. The analysis was done by scanning the sample through a wave number range of 650 – 4000 cm^{-1}; 32 scans at 8cm^{-1}resolution.The broad band that falls in the range of 3400–3300 cm^{-1} is associated with the –OH group. The peaks at 1600 cm^{-1} and 1500 cm^{-1} correspond to the C=C stretching vibration. The peaks at the regions 1300 $cm^{-1}$and 1080 cm^{-1} correspond to the C-O stretching. Generally, the FTIR spectrum for the activated cowpea husk indicated the presence of the hydroxyl functional group, –OH, which might be responsible for the adsorption of Congo red. The –OH group of the adsorbent was protonated due to the low pH of the solution. The presence of the $–SO_3–$ group in Congo red will preferentially favour the protonated –OH group of the cowpea husk to form a hydrogen bond during the adsorption process. However, the FTIR spectra analysis results as seen on table 1 indicate that only minor differences between before and after adsorption of Congo red on activated cowpea husk could be established. Therefore, shift in bands and changes in wavelength between the before and after adsorption of samples indicate that chemical transformation must have taken place during chemical treatment or during pyrolysis.

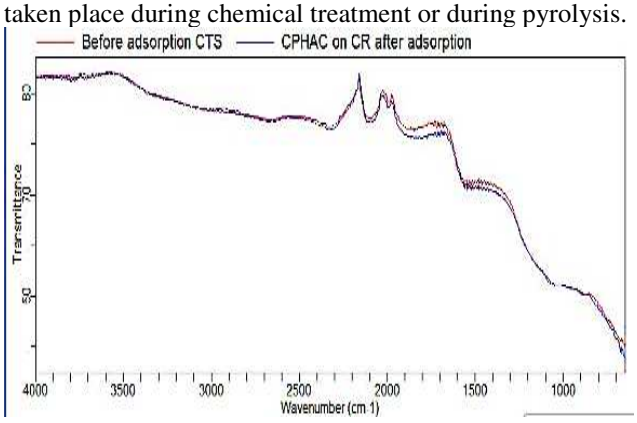

Fig. 2. FTIR spectral of ACPH before and after adsorption of CR

Table 1**.** Different functional group recognized before and after adsorption of CR onto ACPH

Functional group	**Wavelenght class range (cm^{-1})**		
	Before adsorption	**After adsorption**	**Difference**
O-H stretch	3300- 3400 (broad)	-	-
C-H Alkanes	2850- 2960	-	-
	1350- 1470	-	-
C≡C Alkynes	2100- 2260	2113	-15
C=Caromatic	1500-1600	1562	-
C-O	1080-1300	-	-
C-H aromatic	675- 870	873	+4

SEM micrographs of adsorbents before and after adsorption of CR onto ACPH were taken at an accelerating voltage of 15.00 kV and x500 magnification. Fig. 3 shows the surface morphology of CPH before and after activation of CR. It is clear that the surfaces of ACPH are smooth and contains cavities and pores which may enhance adsorption and intra-particle diffusivity [25]. The porous structures have been filled after adsorption of the CR dye. The SEM micrograph of the ACPH before adsorption shows some considerable porous, granular and almost uniform in size where Congo red could be adsorbed with a high probability.

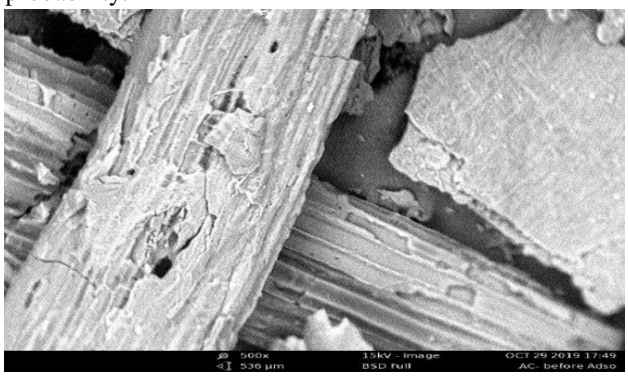

Fig. 3a**.** SEM Micrograph of ACPH before adsorption of CR

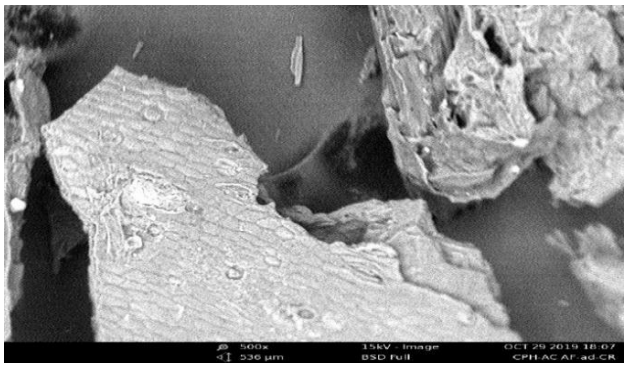

Fig. 3b**.** SEM Micrograph of ACPH after adsorption of CR

3.2 Physical Properties of the Produced Adsorbent

Some of the physical properties of the activated carbon produced are given in table 2. The values of the moisture content, pore volume and the bulk density of the produced activated carbon revealed that it had good adsorptive properties. It was noticed from the properties that, though it might not give up to 100% adsorption but it will be good for adsorption of organic and inorganic materials to a large extent [26].

Table 1. Different functional group recognized before and after adsorption of CR onto ACPH

Adsorbent	**Moisture Content**	**Density**	**Pore Volume**
ACPH	13.6%	0.211g/cm^3	1.79cm^3

3.3 Batch Adsorption

Fig. 4a shows the effect of the amount of ACPH used on the adsorption of Congo red dye. The amount of adsorbent was varied from 0.1 to 0.6 g while the dye concentration was fixed at 50 mg/L. The net quantity of adsorbate removed decreased (from 24.532mg/L to 2.4432mg/L) with increasing mass (0.1g- 0.6g) of ACPH which is attributed to an increase in the sportive surface area and the availability of more active binding sites. The net equilibrium amount adsorbed however is an expression of the efficiency of an adsorbent which may not show increase in the amount adsorbed per unit mass as the adsorbate dose increases [27]. The effect of initial concentration of CR was investigated by varying the concentration from 50 to 500mg/L, at natural pH of dye solution with agitation time and speed of 1hr and 130rpm respectively as reported in Fig. 4b. It is evident from the plot that the amount CR adsorbed by ACPH increases with increasing concentration. At low concentration, the available driving force for transfer of CR molecules onto the adsorbent particle is low. While at high concentration, there is a corresponding increase in the driving force, thereby, enhancing the interaction between the dye molecule in the aqueous phase and the active sites of the adsorbent. As a result of this, there was an increase in the dye uptake as adsorption capacity increases. Similar trends were reported by other authors [28, 29].

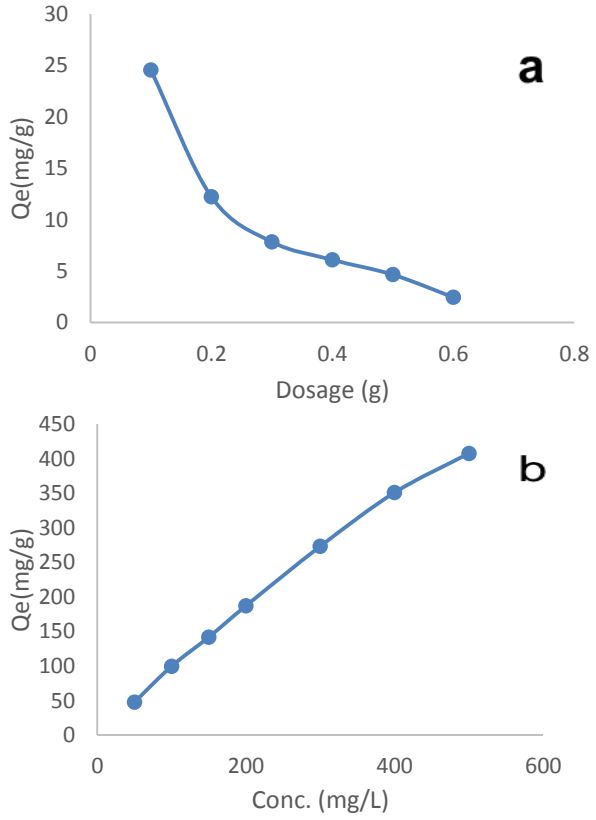

Fig. 4. Effect of (a) adsorbent dosage and (b) initial concentration on the adsorption of CR onto the ACPH.

Fig. 5a showed variation of the amount of CR adsorbed with time onto ACPH. From the plot, it is evident that the rate increased rapidly with time, and then reached equilibrium. The contact time to reach equilibrium was 60min. The adsorption capacity and percent removal of CR onto the adsorbent significantly increased during the initial adsorption stage, and then equilibrium was nearly reached. At this time, removal efficiency reached was 24.3157mg/l for CR. Hence, in the present work, 60 min was chosen as the equilibrium time. However, the removal rate of adsorbate is rapid initially, but it gradually decreases with time until it reaches equilibrium. This can be due to the fact that a large number of vacant surface sites are available for adsorption at the initial stage, and after a lapse of time, the remaining vacant surface sites are not easy to be occupied due to repulsive forces between the solute molecules on the solid and bulk phases. Similar findings were reported by another author [25-30].

As observed in Fig. 5b, the pH plays an important role in the adsorption of Congo red dye on the adsorbents because it influences the surface polarity of the adsorbents, ionic mobility and degree of ionization of the pollutants (Congo Red dye). It is a known fact that when pH of solution is less than pHpzc, the adsorbent surface acquires positive charge and then adsorbs the anionic dye (Congo Red) easily [12-31]. The adsorption of Congo red dye on activated cowpea husk is preferred at pH less than pHpzc of adsorbents, i.e. at neutral and or acidic pH of solution. This suggests that the ACPH has great adsorption capacity in almost neutral media. Its surface polarity and active sites could be blocked by high concentration of H+ or OH- ions hence the adsorption efficiency decreases at very high pH value. This suggests that the active sites and surface polarity of this adsorbent increase in acidic media that enhances the adsorption of dye. To simplify more the adsorption mechanism in the present case it can be concluded that a decrease in the adsorption at higher pH reflect that electrostatic repulsion may occur between the anionic Congo Red dye and negatively charged adsorbent surface under alkaline pH conditions. While under acidic pH (lower pH), concentration of H^+ ion increases and also the adsorbent surface acquires positive charge. Under this condition attractive forces may occur between anionic dye molecule and the positively charged adsorbent surface. At lower pH which causes maximum removal of dye. Furthermore, excess amount of negatively charged hydroxyl ions may also compete with dye molecules for adsorbent sites under higher pH condition (basic pH) and so decrease the adsorption effectiveness of Congo red on adsorbent used.

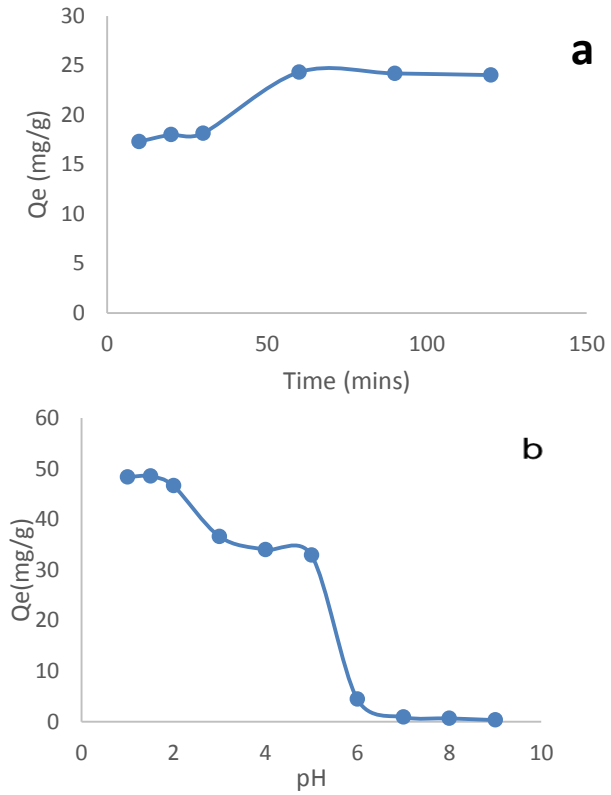

Fig. 5. Effect of (a) Contact time (b) pH of the CV adsorption onto ACPH

3.4 Adsorption Kinetics

(a) The pseudo first-order equation

The pseudo first-order equation is generally expressed as follows [32]:

$$\frac{\partial q_t}{\partial t} = k_1(q_e - q_t) \quad (3)$$

Where q_e and q_t are the adsorption capacity at equilibrium and at time t, respectively (mg·g^{-1}), k_1 is the rate constant of pseudo first-order adsorption (l·min^{-1}). After integration and applying boundary conditions $t = 0$ to $t = t$ and $q_t = 0$ to $q_t = q_t$, the integrated form becomes:

$$\log(q_e - q_t) = \log(q_e) - \frac{k_1}{2.303}t \quad (4)$$

The values of $\log(q_e - q_t)$ were linearly correlated with t which gave a linear relationship from which k_1 and q_e was determined from the slope and intercept of the plot respectively (Fig. 6a).

(b) The pseudo second-order equation

The pseudo second-order adsorption kinetic rate equation is expressed as

$$\frac{\partial q_t}{\partial t} = k_2(q_e - q_t)^2 \quad (5)$$

k_2 is the rate constant of pseudo second-order adsorption (g·mg^{-1}·min^{-1}). For the boundary conditions $t = 0$ to $t = t$ and $q_t = 0$ to $q_t = q_t$, the Integrated form of Eq. (5) becomes:

$$\frac{1}{(q_e - q_t)} = \frac{1}{q_e} + k_t \quad (6)$$

This is the integrated rate law for a pseudo second-order reaction.

The equation can be rearranged to obtain Eq. (7), which has a linear form:

$$\frac{t}{q_t} = \frac{1}{K_2 q_e^2} + \frac{1}{q_e}(t) \quad (7)$$

If the initial adsorption rate, h (mg·g^{-1}·min^{-1}) is;

$$h = k_2 q_e^2 \quad (8)$$

Then eqn (7) becomes

$$\left(\frac{1}{q_t}\right) = \frac{1}{h} + \frac{1}{q_e}(t) \quad (9)$$

The plot of (t/q_t) versus t gave a linear relationship from which q_e and $k_1$were determined from the slope and intercept of the plot respectively (Fig. 6b).

(c) Elovich Equation

The Elovich kinetic model is described by the following relation [33]:

$$q_t = 1/\beta \ln(\alpha\beta) + (1/\beta) \ln t \quad (10)$$

This model gives useful information on the extent of both surface activity and activation energy for adsorption process. The parameters (α) and (β) was calculated from the slope and intercept of the linear plot of q_t versus ln(t) (Fig. 6c).

(d) Intraparticle Diffusion Equation

The slowest step in an adsorption process is usually taken as the rate determining step. This step is often attributed to pore and intra particle diffusion. Since pseudo first and pseudo second order models cannot provide information on effect of intra particle diffusion in adsorption, intra particle diffusion model can be used. Possibility of involvement of intra particle diffusion model as the sole mechanism was investigated according to Weber–Moris equation [34]:

$$q_e = C + k_{int} t_{1/2} \quad (11)$$

Where the constant k_{int}(mg/g min$^{0.5}$) is the intra particle diffusion rate and C is the boundary layer thickness. If the rate-limiting step is only due to the intra particle diffusion, then q_t versus $t_{1/2}$ will be linear and the plot passes through the origin (Fig. 6d).

Table 3. Parameters of the kinetic models for the adsorption of CR onto AC-CPH

Kinetic models	Parameters	Values
Pseudo-first order	q_{eExp}(mg/g)	24.316
	q_{eCal}(mg/g)	11.962
	K_1(min^{-s})	0.037
	R^2	0.850
Pseudo-second order	q_{eExp}(mg/g)	24.316
	q_{eCal}(mg/g)	25.908
	K_2(min^{-s})	0.005
	R^2	0.994
	B	0.298
Elovich	A	0.124
	R^2	0.847
Intra particle diffusion	K_3	1.060
	C	13.705
	R^2	0.841

Table 3 shows kinetic models for the adsorption of CR onto the adsorbent. The pseudo-second-order kinetic model fits the experimental data quite well; the correlation

coefficients values, R^2, up to almost unity, and the experimental and theoretical uptakes are in good agreement. This indicates the applicability of the second-order kinetic model to describe the adsorption process of CR onto the adsorbent.

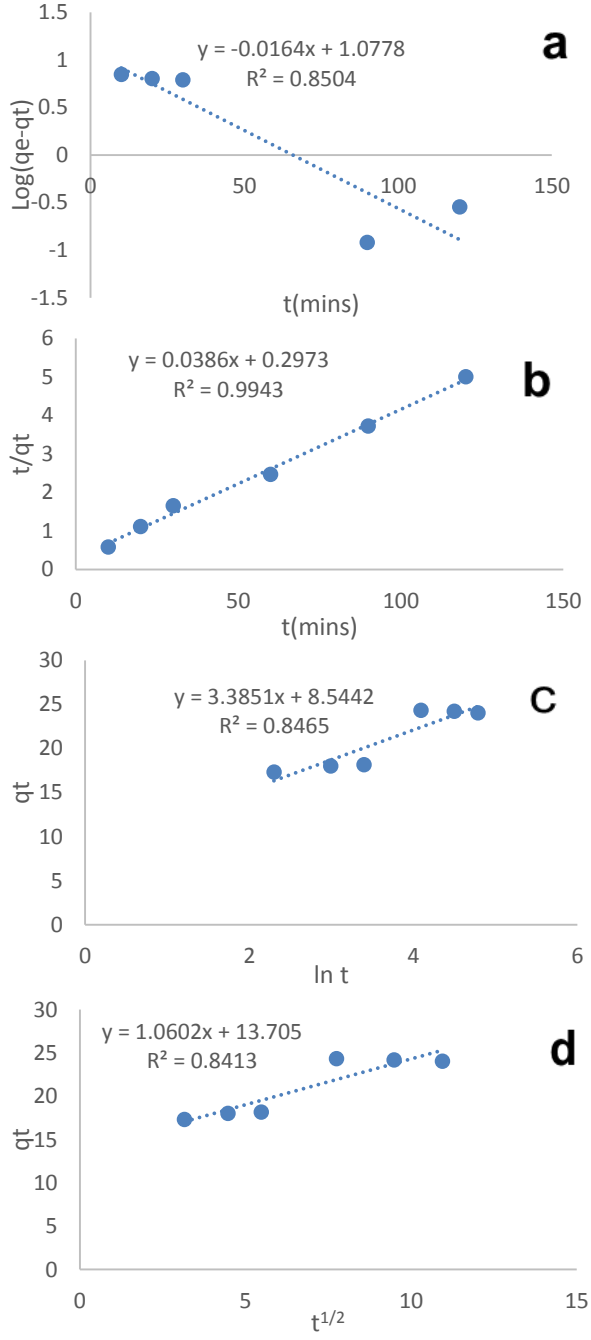

Fig. 6. (a) pseudo-first order (b) pseudo-second order (c) Elovich linear (d) Intra particle diffusion plot for adsorption of CR onto AC-CPH

3.5 Adsorption Isotherm

Adsorption isotherms provide helpful information to identify the uptake mechanism and characteristics of the adsorbent surface for the design of sorption systems [35-36]. Three adsorption isotherm models; Langmuir, Freundlich and Temkin were applied to fit the experimental data for the removal of CR dye by CPH.

(a) Langmuir isotherm

Langmuir theory assumes that adsorbent has a limited adsorption capacity (q_{max}) and adsorbate forms a monolayer on the adsorbent surface where active sites are identical and there are absences of interaction between the adsorbed molecules [37].

Langmuir isotherm is given by the following equation:

$$q_e = \frac{Q_O K_L C_e}{1+K_L C_e} \quad (12)$$

Where:

C_e = the equilibrium concentration of adsorbate (mg/L)

q_e = the amount of dye adsorbed per gram of the adsorbent at equilibrium (mg/g).

Q_o = maximum monolayer coverage capacity (mg/g)

K_L = Langmuir isotherm constant (L/mg).

The values of q_{max} and K_L were computed from the slope and intercept of the Langmuir plot of $\frac{1}{qe}$ versus $\frac{1}{Ce}$.

(b) Freundlich isotherm

Freundlich model [38], is applied in the case of multilayer adsorption. However, this model assumes the existence of interactions between adsorbed molecules. Freundlich isotherm model can be defined by the following equation:

$$Q_e = K_f C_e^{1/n} \quad (13)$$

qe(mg/g) is the adsorbed amount at equilibrium, Ce (mg/L) is the concentration of the adsorbate in the solution at equilibrium, k_f is the Freundlich constant, n is the adsorption intensity.

Its linear form is given by the following equation:

$$\text{Log}Q_e = logkf + \frac{1}{n} logC_e \quad (14)$$

(c) Temkin isotherm

Temkin's model is based on the hypothesis that the heat of adsorption due to interactions with the adsorbate decreases linearly with the recovery rate.

Temkin equation is given by the following expression:

$$q_e = BlnA_T + \text{Bln}C_e \quad (15)$$

Where;

A_T =Temkin isotherm equilibrium binding constant (L/g), b_T = Temkin isotherm constant, R= universal gas constant (8.314J/mol/K), T= Temperature at 298K and B = Constant related to heat of adsorption (J/mol).

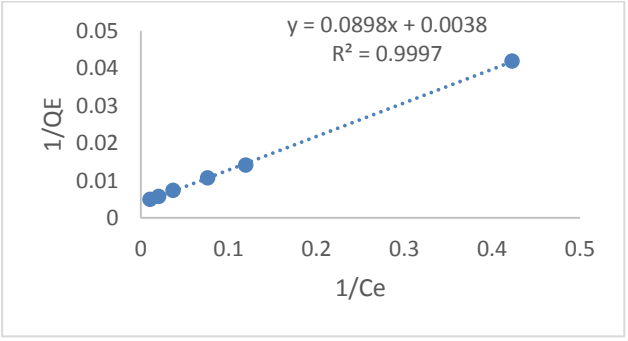

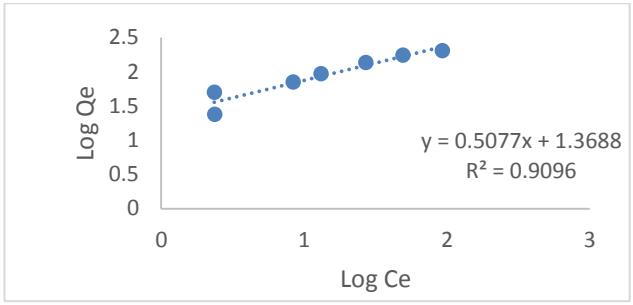

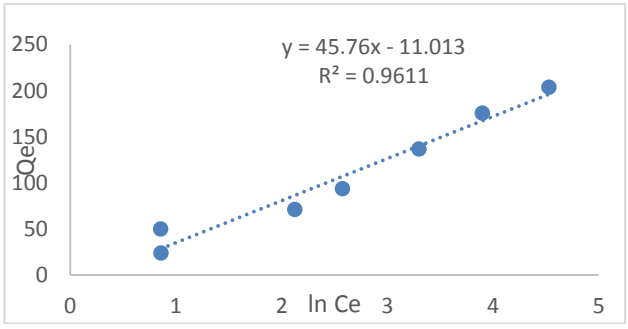

Fig. 6. (a) Langmuir (b) Freunlich (c) Temkin adsorption isotherm of CR onto AC-CPH

The Langmuir, Freundlich and Temkin isotherm constants are presented in Table 4. From Table 4, it can be observed that the regression correlation coefficient (R^2) of the Langmuir equation (R^2 = 0.999) is higher when compared with that of the Freundlich equation (R^2 = 0.909) and the Temkin equation (R^2 = 0.961), implying that the adsorption isotherm data are well fitted by the Langmuir isotherm. The fact that the Langmuir isotherm fits the experimental data very well may be due to the homogeneous distribution of active sites on the ACPH surface because application of the Langmuir equation involves the assumption that the surface is homogeneous.

Table 4. Isotherm Constant for the adsorption of CR onto Activated Cowpea husk

	Langmuir		
Qmax	K_L(L/mg)	R^2	
263.16	0.999	0.999	
	Freundlich		
1/n	N	K_f	R^2
1.969	0.508	23.38	0.909
	Temkin		
A	B	R^2	
0.787	45.96	0.961	

3.6 Thermodynamics

Thermodynamic parameters of adsorption were determined from the experimental results obtained at different temperatures using the following equations:

$\Delta G = \Delta H - T\Delta S$ (16)

Where T(K) is solution temperature

$K_d = qe/Ce$ (17)

Where K_d is the distribution coefficient, qe (mg/g) is the adsorption capacity at equilibrium, Ce(mg/L) is the solution concentration at equilibrium.

The standard enthalpy ΔH and entropy ΔS were determined from the following equation of Van't Hoff:

$\ln k_d = -\Delta G/RT = -(\Delta H/RT) + (\Delta S/R)$ (18)

Where R is the universal gas constant.

ΔH and ΔS were obtained from the slope and the intercept of the plot of $\ln(K_d)$ as a function of 1/T respectively. Thermodynamic parameters obtained are summarized in Table 5. The values of Gibbs free energy (ΔG) of adsorption of CR adsorption on ACPH were found to be negative corresponding to a spontaneous process [39]. The positive value of ΔH confirms that adsorption phenomenon of CR on ACPH is endothermic. The negative value of ΔS indicates that the order of distribution of the dye molecules on the adsorbent is high compared to that in the solution. This also suggests the probability of a thermodynamically favourable adsorption [40].

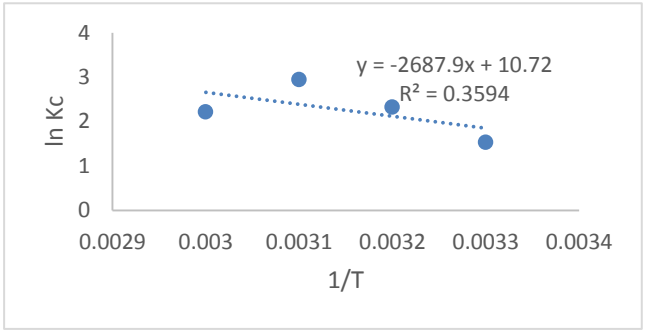

Fig 7. Van`t Hoff plot for adsorption of CR onto AC-CPH

Table 5. Thermodynamics Parameter of CR Adsorption on Activated Cowpea Husk

T (K)	Qe (mg/g)	ΔG (kJ/mol)	ΔH (kJ/mol)	ΔS (J/mol.K)
303	41.096	-3852.78	286.34	-0.0053
313	45.533	-6041.72		
323	47.495	-7902.12		
333	45.095	-6141.78		

3.7 Comparison with other studies

Table 6 illustrates the comparison of adsorption capacities of CR by various adsorbents. As observed, the maximum monolayer uptake capacity (Qm, mg/g) of ACPH was above the other types of sorbents. Thus, this adsorbent can be considered as an effective option for the removal of CR from aqueous media.

Table 6. Comparison of the maximum sorption capacity of ACPH with other adsorbents for adsorption of Congo red.

Adsorbent	Q_{max} (mg/g)	Reference
Eichhornia	1.58	[41]
Activated carbon (Laboratory grade)	1.88	[42]
Cashew nutshell	5.18	[43]
Bagasse fly Ash	11.89	[44]

Montmorillonite	12.70	[45]
Cattail root	38.79	[46]
Neem leaf powder	41.20	[47]
Raw Cowpea husk powder	161.29	[24-48]
Activated Cowpea husk powder	263.16	This study

4. Conclusion

The search for an alternative low-cost and environmentally friendly adsorbent, suitable for the removal of toxic dyes from contaminated wastewater provided the impetus for this research work. Activated Cowpea husk (ACPH) was used for the adsorption of Congo Red dye under different experimental conditions. The adsorption efficiency was prominently affected on changing the experimental conditions. Comparative adsorption studies showed that maximum adsorption of Congo Red dye at pH1.5 on the surface of ACPH was investigated as 24.26mg/g. This shows that ACPH has a great adsorption efficiency for Congo red dye due to its surface polarity and greater number of active sites. Thermodynamic studies revealed that the adsorption process is spontaneous. The negative value of ΔS (-0.0053J/mol. K) infer that the randomness decreases at the adsorbent/adsorbate interface during the adsorption process. The kinetics studies indicated that the adsorption of Congo Red dye on this adsorbent follow pseudo-second order model better than pseudo-first order model with a correlation coefficient, R^2 (0.994) almost up to unity. The equilibrium data for the adsorption of dye on this adsorbent was tested with various adsorption isotherms such as Langmuir, Freundlich, and Temkin models. However, the data fits the Langmuir which indicates that it possesses heterogeneous surface with non-uniform adsorption sites and multilayer formation.

Acknowledgement

The authors wish to thank all technical staff of Chemistry Laboratory, Department of Pure and Industrial Chemistry, Bayero University, Kano, Nigeria for the assistance they rendered during the course of this research.

Conflict of Interest

The authors declare that they have no conflict of interest

References

[1] Upadhye, G. R. (2016). Analytical study of agricultural waste as non conventional low cost adsorbent removal of dyes from aqueos solutions. International J. Chem. Studies,. 128-133.

[2] Akinola, L. I. (2016). Kinetics and equilibrum studies of congo red adsorption on adsorbent from bambara groundnut hulls. Al-Hikmah Journal of Pure and Applied sciences, 79-88 .

[3] Alkaim, A. F., Sadik, Z., Mahdi, D. K., Alshrefi, S. M., Al-Sammarraie, A.M., Alamgir, F. M., Singh, P. M., Aljeboree, A. M. (2015). Preparation, structure and adsorption properties of synthesized multiwall carbon nanotubes for highly effective removal of maxilon blue dye. Korean J. Chem. Eng. 32, 2456–2462.

[4] Rani, K. C., Naik, A., Chaurasiya, R. S., Raghavarao, K. (2017). Removal of toxic Congo red dye from water employing lowcost coconut residual fibre. Water Science and Tech. 75(9), 2225-2236.

[5] El-Messaoudi, N., El-Khomri, M., Chlif, N., Chegini, Z. G., Dbik, A., Bentahar, S., Lacherai, A. (2021). Desorption of Congo red from dye-loaded phoenix dactylifera date stones and ziziphus lotus jujube shell. Groundwater for Sustainable Dev. 12, 100552.

[6] Rehman, R.,. Manzoor. I., Mitu, L. (2018). Isothermal study of Congo red dye biosorptive removal from water by solanum tuberosum and pisum sativum peels in economical way. Bulletin of the Chem. Society of Ethiopia, 32(2), 213-223.

[7] Stjepanovic, M., Velic, N., Galic, A., Kosovic, I., Jakovljevic, T., Habuda-Stanic, M. (2021). Removal of Congo Red from Waste Wood Biomass. Water, 13, 279.

[8] El-Naggar, N. E., Rabei, N. H., El-Malkey, S. E. (2020). Eco-friendly approach for biosorption of Pb2+ and carcinogenic Congo red dye from binary solution onto sustainable Ulva Lactuca biomass Scientific Reports, 10, 16021.

[9] Adelaja, O. A., Bankole, A. C., Oladipo, M. E., Lane, O. B. (2019). Biosorption of Hg(II) ions, Congo red and their binary mixture using raw and chemically activated mango leaves. International Journal of Energy and Water Resources, 3(1), 1-12.

[10] Wu, J., Yang, J., Feng, P., Huang, G., Xu, C., Lin, B. (2020). High-efficiency removal of dyes from wastewater by fully recycling litchi peel biochar. Chemosphere, 246, 125734.

[11] Zheng, H., Sun, Q., Li, Y., Du, Q. (2020). Biosorbent prepared from pomelo peel by hydrothermal technique and its adsorption properties for congo red. Materials Research Express, 7(4), 045505.

[12] Wu, J., Zhang, Z., Xu, J., Lu, X., Wang, C., Xu, H. Yuan, H., Zhang, J. (2020). Adsorption of Congo red by BG. Bioresources, 15(3) 6928-6940.

[13] Yu, H., Wang, T., Yu, L., Dai, W., Ma, N., Hu, X., Wang, Y. (2016). Remarkable adsorption capacity Ni-doped magnolia leaf derived bio adsorbent for Congo red Journal of the Taiwan Institute of Chemical Engineers, 64, 279-284.

[14] Dai, H., Huang, Y., Zhang, H., Ma, L., Huang, H., Wu, J., Zhang, Y. (2020). Direct fabrication pf hierarchically processed pineapple peel hydrogels for efficient congo red adsorption. Carbohydrate Polymers, 230, 115599.

[15] Mondal, N. K., Kar, S. (2018). Potentiality of banana peel for removal of Congo red dye from aqueous solution: isotherm, kinetics and equilibrium studies Applied Water Science, 8(6) 1-12.

[16] Ojo, T. A., Ojedokun, A. T., Bello, O. S. (2019). Functionalization of powdered walnut shell with

orthophosphoric acid for Congo red removal. Particulate Science and Technology, 37(1), 74-85.
[17] Litefti, K., Freire, M. S., Stitou, M., Gonzalez-Alvarez, J. (2019). Adsorption of an anionic dye (Congo red) from aqueous solutions by pine bark, Scientific Reports, 9(1), 1-11.
[18] Tyagi, U. (2020). Adsorption of dyes using activated carbon derived from pyrolysis of vetiveria zizanioides in a fixed bed reactor. Groundwater and Sustainable Development, 10, 100303.
[19] Wekoye, J. N., Wanyonyi, W. C., Wangila, P. T., Tonui, M. K. (2020) Kinetic and Equilibrium studies of Congo red dye adsorption on cabbage waste powder. Environmental Chemistry and Ecotoxicology, 2, 24-31.
[20] Abdul, M., Abbas, K., Natasha, A., Muhammed N., (2020). Adsorption of Congo red dye on rice husk, rice husk char and modified rice husk char, Bull. Chem. Soc. Ethiop. 34(1), 53.
[21] Ososanya, T. O., Alabi, B. O., Sorunke, A. O. (2013). Performance and digestibility of corncob and cowpea husk diets by West African dwarf sheep, Pakistan Journal of Nutrition, 12(1), 85-8.
[22] Ash, B., Satapathy, D., Mukherjee, P. S., Nanda, B., Gumaste, J. L., Mishra, B. K. (2006). Characterization and application of activated carbon prepared from coir pith, J. Sci. Ind. Res. 65, 1008-1012.
[23] Sugumaran, P., Priya, V. S., Ravichandran, P., Seshadri, S. (2012). Production and characterization of activated carbon from banana empty fruit bunch and *Delonix regia* fruit pod. Journal of Sustainable Energy & Environment 3, 125-132.
[24] Ayuba, A. M., Idoko, B. (2021). Cowpea husk adsorbent for the removal of crystal violet from aqueous solution. J. Appl. Surf. Interfaces, 9, 9-16.
[25] Adekola, F. A., Abdus-Salam, N., Abdul-Rauf, L. B. (2011). Removal of arsenic from aqueous solution by synthetic hematite. J. Chem. Soc. Nigeria, 36(2), 52–58.
[25] Abdus-Salam, N., Adekola, S. K. (2018). Adsorption studies of zinc (II) on magnetite, baobab (*Adansonia digitata*) and magnetite–baobab composite, Applied Water Science, 28-222 (https://doi.org/10.1007/s13201-018-0867-7.
[26] Liu, Q., Yang, B., Zhang, L., Huan, R. (2015). Adsorption of an anionic azo dye by cross-linked chitosan/bentonite composite. International Journal of Biological Macromolecule, 72, 1129–1135.
[27] Prahas, D., Kartika, Y., Indraswati, N., Ismadji, S. (2008). Activated carbon from jackfruit peel waste by H_3PO_4 chemical activation: pore structure and surface chemistry characterization, Chemical Engineering Journal, 140, 32–42.
[28] Nasuha, N. (2010). Rejected tea as a potential lowcost adsorbent for the removal of Methylene blue. J. Hazard Matters, 15, 175, (1-3), 126-32.
[29] Dalal, Z., Husein, E. A., Maram, B. (2016). Adsorption of cadmium (II) onto watermelon rind under microwave radiation and application into surface water from Jeddah, Saudi Arabia. Arab J Sci Eng. 14, 237-241.
[32] Bergmann, C. P., Machado, F. M. (2015). Carbon nanomaterials as adsorbent for environmental and biological applications, Springer International Publishing, Switzerland.
[33] Sinha, S., Behera, S. S., Das, S., Basu, A., Mahapatra, R. K., Murmu, B. M., Dhal, N. K., Tripathy, S. K., Parhi, P. K. (2018). Removal of Congo Red dye from aqueous solution using Amberlite. Chemical Engineering Communications, 205(4), 432-444.
[34] Ali, N., Said, A., Ali, F., Raziq, F., Ali, Z., Bilal, M., Reinert, L., Begum, T., Iqbal, H. M. N. (2020). Cr(vi) Removal from aqueous solition using a Magnetite snail shell. Water, Air, Soil Pollution, 231(50), 1-16.
[35] Din, A. T. M., Hameed, B. H., Ahmad, A. L. (2009). Batch Adsorption of phenol onto physiochemical activated coconut shell. Journal of Hazardous Materials, 161, 1522-1529.
[36] Omidi-Khaniabadi, Y., Heydari, R., Nourmoradi, H., Basiri, H., Basiri, H. (2016). Low-cost sorbent for the removal of anilineand methyl orange from liquid-phase: Aloe Vera leaves waste. Journal of the Taiwan Institute of Chemical Engineers, 68, 90-98.
[37] Lagergern, S. (1898). About the theory of so-called adsorption of soluble substances. K. Sven. Vetenskapsakad Handl. 24, 1–39.
[38] Freundlich, H. (1926). Colloid and capillary chem. Metheum. London.
[39] Limousin, G., Gaudet, J. P., Charlet, L., Szenknect, S., Barthes, V., Krimissa, M. (2007). Sorption isotherms: a review on physical bases, modeling and measurement. Applied Geochemistry, 22(2), 249-275.
[40] Jain, A. K., Gupta, V. K., Jain, S., Suhas, S. (2011). Removal of chlorophenols using industrial wastes. Environmental Science Technology, 38(4), 1195–1200.
[41] Wanyonyi, W. C., Onyari, J. M., Shiundu, P. M. (2014). Adsorption of Congo Red Dye from Aqueous Solutions using Roots of Eichhornia Crassipes: Kinetic and Equilibrium Studies. Energy Procedia, 50, 862-869.
[42] Mall, I., Srivastava, V., Agarwal, N., Mishra, I. (2005). Removal of Congo red from aqueous solution by bagasse fly ash and activated carbon: kinetic study and equilibrium isotherm analyses. Chemosphere, 61, 492-501.
[43] Kumar, P. S., Ramalingam, S., Senthamarai, C., Niranjanaa, M., Vijayalakshmi, P., Sivanesan, S. (2010). Adsorption of dye from aqueous solution by cashew nut shell Desalination and Water Treatment, 261, 52-60.
[44] Wang, L., Wang, A. (2007). Adsorption characteristics of Congo red onto chitosan/montmorillonite nanocomposite. Journal of Hazardous Materials, 147, 979-985.
[45] Hu, Z., Chen, H., Ji, F., Yuan, S. (2010). Removal of

Congo red from Aqueous solution by cattail root. Journal of Hazardous Materials, 173, 292-297.
[46] Bhattacharrya, K., Sharma, A. (2004). Azadirachta indica Leaf powder as an effective biosorbent for Dyes. Journal of Environmental Management, 71, 217-229.
[47] Lian, L., Guo, L., Guo, C. (2009). Adsorption of Congo Red from aqueous solutions onto Ca-bentonite. Journal of Hazardous Materials, 161, 126-131.

Recommended Citation
Ayuba, A. M., Idoko, B. (2021). Kinetics, Equilibrium and Thermodynamics Studies of Congo red dye Adsorption fromAqueous Solution onto Activated Cowpea (*Vigna Unguiculata)* Husk. *Algerian Journal of Chemical Engineering*, . 02, 66-75. http://dx.doi.org/ 10.5281/zenodo.5670200